

H. BATUHAN OZTEMEL
 INCI SALT
 YAVUZ SALT

Department of Chemical
 Engineering, Faculty of Chemical
 and Metallurgical, Yildiz
 Technical University, Istanbul,
 Turkey

SCIENTIFIC PAPER

UDC 502/504:546.2.264-31:662

CARBON DIOXIDE UTILIZATION: PROCESS SIMULATION OF SYNTHETIC FUEL PRODUCTION FROM FLUE GASES

Article Highlights

- Capacities were assumed regarding the emissions and number of industrial power plants worldwide
- Asymmetric polyethersulfone hollow fiber membrane separates CO₂ and N₂ gases from flue gas
- Sulfurization, reverse water-gas shift, and Fischer-Tropsch reactions separate the flue gas
- The synthetic fuel produced is mainly composed of hydrocarbons such as methane, ethane, and butane
- Each cost of equipment is calculated in the profitability analysis

Abstract

Environmental problems are on the rise and nowadays more climate-related, caused primarily by greenhouse gas emissions. Also, worldwide industrial emissions from power plants will cause 50% of the carbon dioxide concentration in the atmosphere by 2035. The simulation study of the synthetic fuel production from flue gas emitted by industrial power plants uses the ChemCAD Software. The study aims to reproduce all flue gas constituents into valuable products to reduce the effects of harmful gases on the environment. The synthetic fuel produced consists of 94.75% hydrocarbons with carbon numbers ranging from 1 to 4 with a 6.59% overall conversion rate. 95% of the sulfur content in flue gas is collected by desulfurizing the fuel mixture. The membrane process also recovers 90.3% of the nitrogen gas in the flue gas. Sulfurization, Reverse Water Gas-Shift, and Fischer-Tropsch syntheses have 95%, 79%, and 98.4% single-pass conversions, respectively, with appropriate catalysts. Economic analysis is also performed, and the payback period of the project is 6.1 years, while the return-on-investment rate is 16.64%.

Keywords: carbon dioxide, Fischer-Tropsch synthesis, flue gas, process simulation, synthetic fuel.

Especially in recent decades, the world has been facing critical environmental problems, such as global warming and depletion of the ozone layer, according to the UN Environment Annual Report 2019 [1]. Besides, acidification in oceans has increased and already affects many ocean species [2]. These environmental issues typically result from carbon dioxide, a well-

known greenhouse gas.

Global warming is the continuous increments in the average temperature of the Earth's climate system due to anthropogenic impacts, for instance, the emission of greenhouse gases such as CO₂, CH₄, NO_x, CF₄, etc. [3,4]. Besides, the global temperature continuously increased after the 1880s. The CO₂ increase mainly caused this growth trend. The usage of heavy-duty machines during the industrial revolution was the key point of these rises. Nonetheless, CO₂ has no direct pay-off on the ozone layer, unlike CFCs (Chlorofluorocarbons) and HFCs (Hydrofluorocarbons). However, higher levels of CO₂ have an indirect pay-off on the ozone layer, as said by the Minnesota Pollution Control Agency [5]. The objective of the ozone layer is

Correspondence: Y. Salt, Department of Chemical Engineering, Faculty of Chemical and Metallurgical, Yildiz Technical University, Davutpasa Campus, 34220 Esenler-Istanbul, Turkey.
 E-mail: salt@yildiz.edu.tr
 Paper received: 25 October, 2021
 Paper revised: 13 March, 2022
 Paper accepted: 21 April, 2022

<https://doi.org/10.2298/CICEQ211025005B>

the filtration of the sunlight. According to the measurements, large holes in the ozone layer critically affect living creatures and nature, glaciers, and oceans by Gunduz [6]. Severe forest fires in the last decade, such as the Australian wildfires in 2020, are also the drawbacks of these anthropogenic applications. Furthermore, oceans perform a vital role in transferring CO₂ into the atmosphere. Over the past 200 years, the oceans have absorbed about half of the CO₂ emitted by anthropogenic applications, as reported by Kolieb and Herr [7].

Emission growth and past solutions

According to Bereiter *et al.* [8], CO₂ concentrations in the atmosphere did not exceed 300 ppm for the last 800,000 years. However, it is well over 400 ppm today and keeps increasing. Hence, today's concentrations are the highest for at least 800,000 years. Since the beginning of the industrial revolution, global CO₂ concentration in the atmosphere has increased. The primary reason for the increment was the growth of heavy-duty machines. These industrial machines were notably beneficial during the industrial revolution. However, they were discharging a high amount of CO₂. The prediction of the CO₂ concentration of each region between 2000 and 2035, using the statistical approach conducted for the input assumption, is shown in Fig. 1. Asia region has had the highest emission rate since the 2000s. The exponential smoothing technique was used for all forecasts in this study to predict possible CO₂ concentrations in different segments. The predictions show these emission rates will consistently increase. Therefore, the CO₂ increment must be solved globally since it threatens the whole ecology. This trend is mainly caused by the increasing energy demand and global fossil fuel consumption. Natural gas, which meets one-third of total energy demand, is the fastest-forming fossil fuel and generates the highest carbon emissions worldwide, as Ozturk and Dincer [9] said. As IEA (International Energy Agency) Statistics [10] reported, a major part of the CO₂ discharge comes from flue (or stack) gases released excessively from industrial power plants.

A few principal areas contribute to worldwide CO₂ emission: agriculture, buildings, industrial power plants, transportation, land use, and forestry. For example, the emissions caused by only industrial power plants at the beginning of the 2000s were 22% of all kinds of CO₂ emissions.

However, this percentage will be approximately 41% by 2035. Besides, G20 countries were responsible for around 80% of these emissions [11]. The highest CO₂ industrial emissions from power plants (excluding

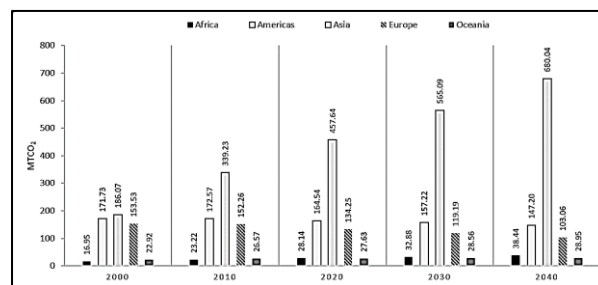


Figure 1. Prediction of CO₂ concentration by region (MtCO₂e/year). (Reproduced from IEA Statistics [10]).

buildings, transportation, and other fugitive emissions) of all G20 countries were recorded by China. It was followed by the United States and the EU [12].

Flue gas (or exhaust gas) is the gas that emits from power plants and includes the reaction outputs of combustion air and residual substances such as particulate matter (dust), sulfur oxides, nitrogen, and carbon monoxide [13]. Facilities that operate with high energy duties and emit excessive flue gas will be the focal point of this study since the CO₂ percentage in typical flue gas is relatively high. Many studies have treated flue gas as a waste of mist at high temperatures, such as oxyfuel combustion and chemical looping, namely carbon capture techniques. There are different techniques to reduce CO₂ emissions, such as boosting renewable energies, applying regulations on CO₂ emission, treating CO₂ as raw material, enhancing plant efficiency to be more energy-saving, or applying carbon capture and storage (CCS) technology. Renewable energies still need to be developed to compete economically with fossil fuels. Novel implementations and usages of sustainable fossil fuels require an integration of the CCS technologies regarding the increasing global energy demand [14]. CCS involves catching the CO₂ at its emission sources, such as coal, petroleum, or natural gas, and transporting it to storage. Oxyfuel combustion is one of those techniques. In this technology, fuel is burned utilizing an oxidizer mixture of pure oxygen and recycled flue gases, comprised mainly of CO₂ and H₂O. The process results in high CO₂-concentrated exhaust gas, which facilitates the capture process of CO₂ after H₂O condensation [15]. Therefore, flue gas can be used as the oxyfuel propagator, as Liang *et al.* [16] stated. The distinguished CO₂ and H₂O gases from the recycled flue gas were used as a diluent to control the temperature in the oxyfuel system. In this regard, the objective is to achieve high-efficiency power generation with low-cost carbon capture. Another common technique is chemical looping which has the same working principle as the oxyfuel method. Chemical looping or chemical looping combustion has no direct contact with air or fuel. It is a method that provides the CCS without vital efficiency or cost penalties. Oxygen

is extracted from the air and then reacts with the hydrocarbon fuel, producing exhaust gases mainly composed of CO₂ and H₂O gases. The water vapor condenses from the gas resulting in a near 100% CO₂ stream [17]. Osman *et al.* [18] have reviewed three aspects of the pressurized operation of chemical looping processes, which create the basis for power and chemical production with integrated CO₂ capture. Pressurized operation of the chemical looping process is essential to maximize thermodynamic and economic performance.

Besides these techniques, biochemical solutions provide the world with a more sustainable future, such as microalgae technology to capture CO₂ from flue gases. Vuppaladadiyam *et al.* [19] suggest that using microalgae cultivation systems to fix CO₂ from industrial flue gases shows favorable results, owing to its potential for producing value-added products, for instance, biodiesel and bioethanol. Also, Kothari *et al.* [20] focus on the algal biomass production techniques and how to accomplish algal biofuel production in an integrated system provided with CO₂ from power plants and wastewater treatment by suitable microalgal species. However, practical applications of these technologies at an industrial scale require significant research and involve high capital costs, although the long-term benefits cut down these prices.

Negligence and lack of use of byproducts (such as flue gas) lead to the techno-economical failure of the process and cause environmental problems [21]. Therefore, the objective of this study is not only to reduce CO₂ emissions but also to create a sustainable fuel model. In other words, the focal point is to reduce both environmental problems and fuel scarcity.

Flue gas emitted from power plant A (other power plants near our process) is supplied to power plant B (the process in this study) to produce synthetic fuel. Flue gas is then cooled and condensed to distinguish the excess water in power plant B. Most nitrogen separated from the mixture after flowing through the parallel-linked membrane system. The remained mixture was treated with the sulfurization reaction to eliminate sulfur content. Then, the CO₂-rich mixture flowed into the reverse water gas-shift (RWGS) and Fischer-Tropsch (F-T) reactors with hydrogen feed. End-products, such as synthetic fuel, nitrogen, elemental sulfur, and excess water, were obtained at the reactor outlet (preliminary economic analysis was performed to emphasize the feasibility of the design). The produced synthetic fuel is recycled back to power plant A.

Consequently, power plant A does not emit CO₂ to the atmosphere since all flue gases are absorbed by power plant B (the process in this study). Furthermore,

power plant A will require fewer external fuels, such as natural gas or coal, since there is a continuous flow of synthetic fuel to power plant A.

METHODOLOGY AND SIMULATION DETAILS

Facility considerations

Site construction and operations should be installed alongside other industrial power plants. The requirement of being closer to those plants is to reduce the transportation cost. There are two reasons: 1) The flue gas of other industrial facilities must be continuously fed into the process. 2) The synthetic fuel produced should be efficiently delivered to other power plants. The continuous recirculation occurs in the zero-emission, as shown in Fig. 2. In this regard, power plants use an environmental-friendly fuel source with sufficient calorific value. In the meantime, other value-added products will be produced and marketed.

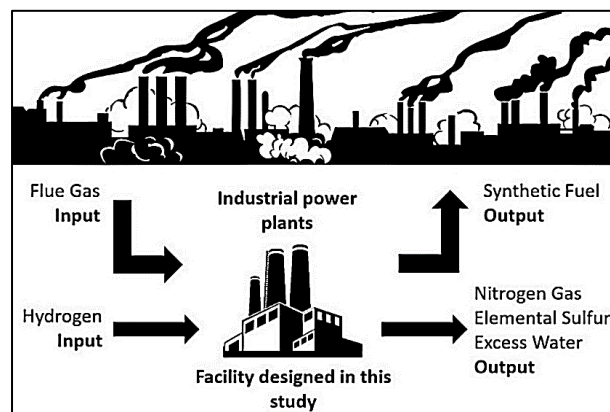


Figure 2. Representation of general perspective.

The inlet flue-gas-flow rate can be estimated by several methods. The mathematical formula of the flow rate by taking the parameters of chimney dimensions was introduced by Ortega [22]. Eq. (1) assumes the flue gas rate in natural ventilation by using a typical chimney's differences in inlet and outlet temperatures. Eq. (1) gives the flue gas flow rate emitted by a chimney, q , in which C_d is the discharge coefficient that is ordinarily taken as 0.65, T_i and T_o are the inlet and outlet temperatures. A is the cross-sectional area of the chimney, and H is the height of the chimney, which were assumed through dimensions of moderate chimney according to Simonovic *et al.* [23].

$$q = C_d A \sqrt{2gH \frac{T_i - T_o}{T_i}} \quad (1)$$

However, the input assumption was achieved using the statistical approach. Based on the CO₂ emission rate of each country and the number of factories in that country, the average amount of flue gas emitted from a typical factory was calculated as approximately 56.46 kilograms per second. According

to the energy type used (gas, coal, renewables, biomass, etc.) by power plants, the CO₂ amount emitted by those factories also changes, and this is also taken into consideration. Since this study aims to encourage environmental-friendly production and consumption, only the gases emitted by coal- and gas-fired plants are involved in the statistical approach. Besides, inlet conditions of flue gases by post-combustion fossil fuel-fired power plants are given in Table 1 [24].

Table 1. Inlet conditions of flue gases (Reproduced from Arachchige and Melaaen [24], with permission from Elsevier)

Flue gas type	Coal-Fired	Gas-Fired
Temperature (°C)	40	40
Pressure (kPa)	110	110
Flow rate (kg/s)	56.46	
Composition	w/w (%)	
H ₂ O	5.08	5.09
N ₂	70.4	75.1
CO ₂	20.6	6.21
O ₂	3.90	13.5
H ₂ S	0.06	0

Process design

The overall process flow diagram is shown in Fig. 3. The excess water in flue gas is first distinguished by flash distillation to provide a non-aqueous mixture for membrane separation. The hollow fiber membranes separated about 95% of the nitrogen, and then the mainstream, which mainly contains CO₂, treated with sulfurization reaction occurred in R-201. Desulfurized CO₂-rich stream combined with hydrogen gas before the reverse water gas shift reactor (R-202). The syngas containing CO and H₂ gases were separated from the unreacted CO₂. The unreacted CO₂ gas was recycled back to combine with the R-202 inlet. Then, highly reactive syngas with 600 °C was involved in the Fischer-Tropsch synthesis in R-203 to produce the synthetic fuel. Throughout the process, the excess water was distinguished and directly bypassed. The process simulated is constituted mainly by hydrocarbon systems, and the pressure of the system is higher than 100 kPa. Thus, Soave-Redlich-Kwong (SRK) equilibrium is used because it is an appropriate thermodynamic equation of state (EOS) for this process [25].

Membrane separation process

Aaron and Tsouris [26] indicate that around 7 gigatons of carbon spread every year. Therefore, the CCS and reduction of CO₂ emissions is an important area of research. There are several methods for CCS: Liquid absorption with a monoethanolamine (MEA)

such as amine scrubbing process, cryogenic distillation, membrane process, pressure- or temperature swing adsorption using various solid sorbents, algae-based uptake, etc. In liquid absorption, CO₂ is obtained and collected in the regeneration column after a solvent is utilized that dissolves CO₂, but not nitrogen gas or any other components in the flue gas. Aaron and Tsouris [26] also concluded that liquid absorption using MEA is a promising technology among these methods; however, the recent developments of membrane technologies produce significant efficiency in the separation of CO₂.

Regarding the complexity, energy consumption, and high capital costs of these technologies, membrane separation is an appropriate capture process due to its high efficiency, easy scale-up, and low energy consumption. Common membranes for CO₂ capture can be summarized as polymeric, inorganic, carbon, and mixed matrix membranes [27]. CO₂ separation using biopolymer-based membranes is one of the new studies in sustainable membrane technologies within the scope of green process engineering [28]. Song *et al.* [29] reported that the polyethersulfone (PES) membranes have excellent stability and high separation performance for CO₂ separation from a gas mixture. Therefore, the membrane module formed by the asymmetric PES hollow fibers is suitable for CO₂ separation. The hollow fiber membrane type was also preferred due to its high membrane surface area and packing density. Due to the CO₂, N₂, and O₂ separation challenge, Song *et al.* [29] used a multiple membrane stage process with four membrane modules linked in a parallel structure to distinguish the components efficiently. However, two membrane modules were combined in the same manner, as shown in Fig. 4.

The general properties of each stream that flowed through both membranes, M-101 and M-102, were summarized in Table 2. In addition, CO₂/N₂ ratio by weight compositions was also given to indicate the performance of the membrane process.

Apart from the membranes, flash separators were used for equilibrium separations. Equilibrium flash separation is typical equipment used in industries, especially in the petroleum industry. A feed stream is separated into liquid and vapor streams in an equilibrium flash vaporization or flash distillation. According to Towler and Sinnott [30], the feed stream to the flash vessel must be in neither liquid nor gas state but in both states. The separation of feed liquid droplets and mists from the gas component is feasible whenever the temperature of the vapor is reduced below the dew point. Thus, the necessary heat must be given to the mainstream or removed from it to bring the stream to

C-101 Feed Compr.	E-101/2 Flue Gas Coolers	V-101 L/V Separator	M-101/2 Membranes	C-102/3 Membrane Compr.	E-103/4 Heaters	V-102/3 L/V Separators	H-101/2/3 Pre-Reactor Furnaces	R-201 Sulfurization Reactor	E-201 Post-Reactor Heater	V-201 Sulfur Separator
R-202 RWGS Reactor	E-202/3 Heaters	R-203 F-T Reactor						V-202/3 L/V Separators	V-204/5 L/V Separators	E-204/5 Coolers

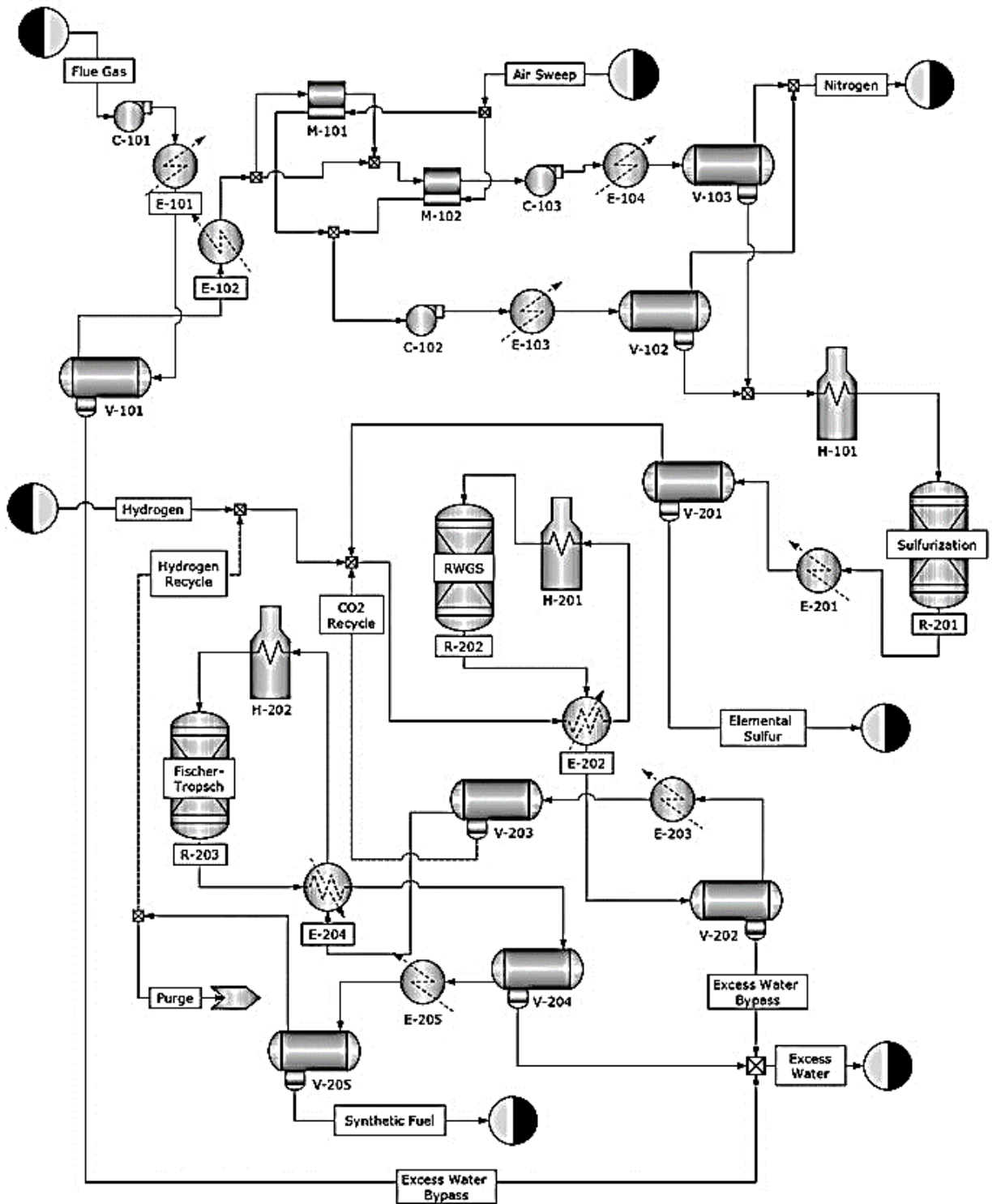


Figure 3. Process flow diagram of the proposed solution.

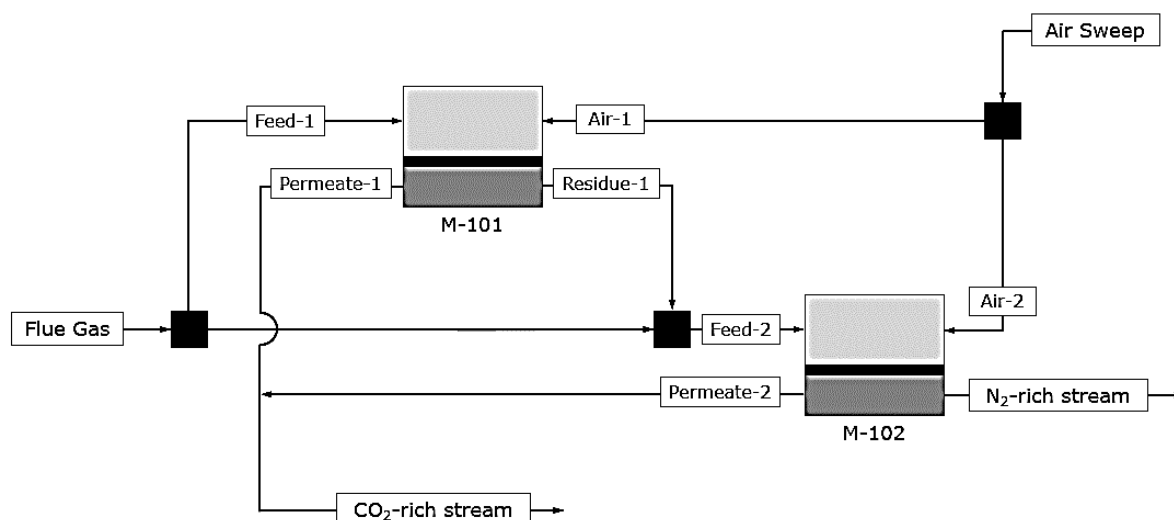


Figure 4. Diagram of the multiple-stage membrane system.

Table 2. Stream properties of the membrane process

	Flue Gas	Feed-1	Permeate-1	Air-1	CO ₂ -rich stream
Flow Rate (kg/s)	53.6	26.8	7.6	0.99	13.8
Temperature (°C)	27	27	17.1	25	17.7
Pressure (kPa)	2000	2000	102.6	202.6	102.6
CO ₂ /N ₂ (w/w)	0.29	0.29	1.74	0	1.58
	Residue-1	Feed-2	Permeate-2	Air-2	N ₂ -rich stream
Flow Rate (kg/s)	20.2	47	6.2	0.99	41.8
Temperature (°C)	26.5	26.4	18.4	25	25.9
Pressure (kPa)	1800	1800	102.6	202.6	1600
CO ₂ /N ₂ (w/w)	0.06	0.18	1.40	0	0.10

suitable "gas-liquid" separation conditions. The composition of the final streams depends on the quantity of the feed vaporized (flashed).

Equilibrium separations require low-temperature levels, whereas the reaction conditions need to be relatively high. As a result, there are increased energy requirements and heat transactions throughout the process. Therefore, heat exchanger selection is essential. Shell and tube heat exchangers are widely used in oil refineries and the petrochemical industry. The fixed tube and type BEM heat exchanger is relatively cost-effective in the petrochemical industry. The operation mechanism of the fixed tube and BEM type exchangers is simple. The setup and repair of these exchangers are also easier [31]. Besides, liquid nitrogen was preferred as a coolant component of coolers, whose working principle is assumed to be a cryogenic operation. Medium-pressure (MP) steam was used as a heater fluid in E-102. Rhine and Truelove

indicated the maximum heat duty allowance for heaters should be between 3 MW and 100 MW. However, the heaters used in the petroleum industry can be around 300 MW or more with 20 MPa maximal pressure [32].

On the other hand, there are three reactors in the process. These reactors were used for sulfurization, the reverse water gas shift, and Fischer-Tropsch synthesis. Simulation and design parameters for each reactor, such as type of reactors, volumes occupied, reaction phase, thermal (or operation) mode and the catalysts used in reactors, and equipment properties in the simulation, are shown in Table 3.

Sulfurization reaction

Sulfur-containing components have destructive impacts on the environment. Hence, the International Organization for Standardization has limited the maximum sulfur content from 3 mg/kg to 500 mg/kg in typical fuels [33].

Table 3. Equipment properties in the simulation

Exchangers	Inlet Temp. °C	Pressure, kPa	ΔT, °C	Type	Heat Duty, MW	Calc. Area, m ²
E-101	707	2000	-702	Fixed-Tube, BEM	-52.32	366.2
E-102	5	2000	22	Fixed-Tube, BEM	1.23	4.3
E-103	276	1000	-406	Fixed-Tube, BEM	-8.9	90
E-104	4	1000	-126	Fixed-Tube, BEM	-7	279.6
E-105	-130	1000	-830	Fixed-Tube, BEM	14.80	103.58
E-201	690	1000	-540	Fixed-Tube, BEM	-7	9.4
E-202	892	1000	-882	Fixed-Tube, BEM	-889.5	1773
E-203	10	1000	-180	Fixed-Tube, BEM	-171.5	1167.3
E-204	600	1000	-595	Fixed-Tube, BEM	-584.7	1569.3
E-205	5	1000	-205	Fixed-Tube, BEM	-190.7	2068
Reactors	Temp. °C	Pressure, kPa	Reaction(s)	Type	Mode	Calc. Volume, m ³
R-201	691	1000	Sulfurization	Equilibrium	Adiabatic	1.5
R-202	892	1000	RWGS	Shift	Adiabatic	20.2
R-203	600	1000	Fischer-Tropsch	Equilibrium	Isothermal	389.4
Membranes	Press, kPa	Flow Pattern	Fiber Length, m	Type	No. of Fibers	Surface Area, m ²
M-101	2000	Counter Current	1.5	Hollow Fiber	10000	21.99
M-102	1800	Counter Current	1.5	Hollow Fiber	10000	21.99
Compressors	Temp, °C	Efficiency, %	ΔP, kPa	Type	Actual Power, MW	
C-101	150	80	1890	Reciprocating	36.23	
C-102	18	80	897	Reciprocating	3.52	
C-103	26	80	600	Reciprocating	-1.25	
Furnaces	Inlet Temp. °C	Pressure, kPa	ΔT, °C	Type	Heat Duty, MW	
H-101	-130	1000	830	Process Heater	14.81	
H-201	-169	1000	1069	Process Heater	1066	
H-202	-170	1000	770	Process Heater	741.4	
Separators	Temp, °C	Pressure, kPa	Product Separated	Type		
V-101	5	2000	Excess H ₂ O	Flash Distillation		
V-102	-130	1000	Liquid N ₂	Flash Distillation		
V-103	-130	1000	Liquid N ₂	Flash Distillation		
V-201	150	1000	Elemental S ₂	Flash Distillation		
V-202	10	1000	Excess H ₂ O	Flash Distillation		
V-203	-170	1000	Excess CO ₂	Flash Distillation		
V-204	5	1000	Excess H ₂ O	Flash Distillation		
V-205	-200	1000	Synthetic Fuel	Flash Distillation		

On the other hand, hydrogen sulfide content in typical flue gas (Table 1) was substantial at 0.1%. Thus, the elemental sulfur was produced in R-201 to distinguish sulfur from the stream. The formation of sulfur from hydrogen sulfide is an essential industrial method to dispose of H₂S. The reaction was shown

in Eq. (2).



Eventually, a high amount of H₂S was converted into solid-state sulfur. However, Mashapa *et al.* [34] indicate the selectivity of the H₂S was highly consider-

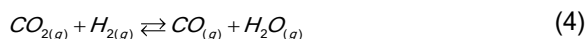
able in a mixture. On this basis, the reaction can occur at about 95% single-pass conversion at 700 °C in the presence of molybdenum disulfide (MoS₂) and tungsten disulfide (WS₂) catalysts. Furthermore, the conversion at higher temperatures was correlated with a reaction rate equation, as shown in Eq. (3) [35].

$$r_{H_2} = k_{H_2S,1}c_{H_2S} - k_{H_2S,2}c_{H_2}^2 \quad (3)$$

The equilibrium constant for H₂S decomposition, k_{H_2S} , was given in Table 4 and modeled in the simulation reactor R-201.

Reverse water gas-shift reaction (RWGS)

The selection of the catalyst in RWGS is important because carbon monoxide is an active molecule. It may directly react back to CO₂ since RWGS is a typical equilibrium reaction shown in Eq. (4).



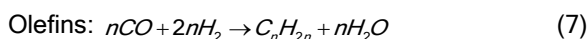
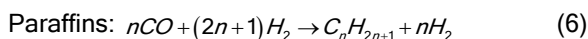
Wolf *et al.* investigated that the reverse water gas shift reaction (RWGS) occurred in the R-202 via a commercial Ni-Al₂O₃ steam reforming catalyst which was produced with 11% Ni (w/w) and a BET (Brunauer-Emmett-Teller) surface area of 7 m²g⁻¹ [36]. Their work shows the catalyst can catalyze the RWGS reaction effectively, and the conversion of 79% at 900 °C is achieved in a short residence time of less than 100 ms. Experiments at varying temperatures and concentrations of CO₂ and H₂ indicate that the power-law rate shown in Eq. (5) for the RWGS was derived. c in which the f letter denotes the forward reaction. The conversion of CO₂ to CO with rate $r_{CO_2,f}$ was shown in Eq. (5), in which f indicates the forward reaction [36].

$$r_{CO_2,f} = K_{RWGS,f}(T)c_{CO_2}c_{H_2}^{0.3} \quad (5)$$

The equilibrium constant for RWGS reaction, K_{RWGS} , was given in Table 4 and modeled in the simulation reactor R-202.

Fischer-Tropsch Synthesis

Syngas, namely carbon monoxide and hydrogen, flowed out from the RWGS reaction and were treated in the Fischer-Tropsch reactor, namely R-203. Fischer-Tropsch synthesis is the fundamental operation in the process where all carbon monoxide and hydrogen react to form hydrocarbon molecules via FeCuK/Al₂O₃ catalyst [37,38]. The Fischer-Tropsch synthesis that involves the catalytic conversion of synthesis gas into a mixture of hydrocarbons (i.e., paraffins, olefins) is shown in Eqs. (6), (7) [39].



The n value stated in Eq. (6) and (7) may be

between 1 and 12 (The hydrocarbons produced vary from C1 to C12+) over FeCuK/Al₂O₃ catalyst during F-T synthesis in the simulation. However, the cetane number and the fuel quality decrease as the number of carbon atoms in the hydrocarbon chain increases. Therefore, the production of hydrocarbons with high carbon numbers is undesired.

Kang *et al.* [37] pointed out that the number of carbon atoms in hydrocarbon molecules can be limited with C4 as long as the reactor temperature increases to 600 °C. Thus, the n value stated in Eq. (6) and (7) can be altered between 1 and 4 in the simulation model. Wang *et al.* [40] carried out a set of kinetic experiments of Fischer-Tropsch synthesis over industrial Fe-Cu-K catalysts. The simplified forms of reaction rates were given in Eq. (8), (9), and (10), where α is the chain growth factor for the carbon number of n , P is the partial pressure of a component, and β is the re-adsorption factor of 1-olefin with a carbon number of n [40].

$$r_{CH_4} = \frac{K_{FT}P_{H_2}\alpha_1}{1 + \left(\frac{1 \cdot P_{H_2O}}{K_{FT}^3 \cdot P_{H_2}^2} + \frac{1}{K_{FT}^2 \cdot P_{H_2}} + \frac{1}{K_{FT}} \right) \sum_{i=1}^N \left(\prod_{j=1}^i \alpha_j \right)} \quad (8)$$

$$r_{C_nH_{2n+1}} = \frac{K_{FT}P_{H_2} \prod_{j=1}^n \alpha_j}{1 + \left(\frac{1 \cdot P_{H_2O}}{K_{FT}^3 \cdot P_{H_2}^2} + \frac{1}{K_{FT}^2 \cdot P_{H_2}} + \frac{1}{K_{FT}} \right) \sum_{i=1}^N \left(\prod_{j=1}^i \alpha_j \right)} \quad (9)$$

where $n \geq 2$

$$r_{C_nH_{2n}} = \frac{K_{FT}(1-\beta_n) \prod_{j=1}^n \alpha_j}{1 + \left(\frac{1 \cdot P_{H_2O}}{K_{FT}^3 \cdot P_{H_2}^2} + \frac{1}{K_{FT}^2 \cdot P_{H_2}} + \frac{1}{K_{FT}} \right) \sum_{i=1}^N \left(\prod_{j=1}^i \alpha_j \right)} \quad (10)$$

where $n \geq 2$.

Eq. (8) is the reaction rate equation of CH₄, in which n is 1. In Eqs. (9) and (10), reaction rates of paraffins and olefins were given for n -values equal to or greater than 2. The equilibrium constant for Fischer-Tropsch synthesis, K_{FT} , was shown in Table 4 and modeled in the simulation reactor R-203.

RESULTS AND DISCUSSION

Simulation analysis

Capacity distributions of the process are given in Table 5. Hence, 7.3 kg of synthetic fuel, 78 kg of nitrogen gas, and 53 grams of solid-state sulfur were produced, and 21 liters of excess water were separated from every 100 kg of flue gas emitted. The nitrogen stream has approximately 95% purity. The other 5% is oxygen. Besides, the excess water stream had 99.98% purity of H₂O, and the elemental sulfur was separated with 99.9% purity.

The n value stated in Eq. (6) and (7) alters between

Table 4. Equilibrium data of chemical reactions [35,36–38]

$$\text{R-201} \quad K_{H_2S} = \exp \left[5.677 - 0.072T + 1.108 \cdot 10^{-4}T^2 + \frac{1549.159}{T} - 0.144 \ln(T) \right] \quad (11)$$

$$\text{R-202} \quad K_{RWGS} = \frac{1}{\exp(-0.294Z^3 + 0.635Z^2 + 4.178Z + 0.317)}, \text{ with } Z = \frac{1000}{T[K]} \quad (12)$$

$$\text{R-203} \quad K_{WGS} = \frac{5078.005}{T} + 5.897 - 13.959 \cdot 10^{-4}T - 27.593 \cdot 10^{-8}T^2 \quad (13)$$

1 and 4 in the simulation model. Hence, the produced fuel mixture at the end of R-203 includes methane, ethane, propane, propylene, butane, and butene. Conversion rates of hydrocarbons are shown in Table 6.

Table 5. Flow rates of mainstreams

Components	Mass Flow Rate (kg/s)
Synthetic Fuel	4.05
Rich-Nitrogen	44.0
Excess Water	11.9
Elemental Sulfur	0.03
Inlet Flue Gas	56.46
Hydrogen Gas Feed	5.0

Table 6. Selectivity distribution over FeCuK/Al₂O₃ catalyst

Catalyst	FeCuK/Al ₂ O ₃
Temperature (°C)	600
CO conversion (%)	98.4
Selectivity (C-mol %)	
CO ₂	12.0
Hydrocarbons	88.0
Hydrocarbon selectivity (%)	
C ₁	29.3
C ₂	15.5
C ₃	23.8
C ₃₌	0.10
C ₄	16.9
C ₄₌	2.40

Natural gas has a great gross heating value compared with other fossil fuels, and it is a widespread fuel type regarding its great amount of light hydrocarbon content [41]. Light hydrocarbons release more energy because they contain more hydrogen atoms than heavier hydrocarbons. Also, natural gas is a non-toxic fuel type since it contains sulfur in small quantities. Since the synthetic fuel produced during this study is an alternative energy source to fossil fuels, the compositional benchmark of synthetic fuel and natural

gas is shown in Table 7. Desulfurized energy utilization is important for the environment. The produced synthetic fuel does not contain any sulfur composition, whereas a typical natural gas may contain hydrogen sulfide. However, synthetic fuel contains relatively low methane compounds, which lowers the calorific value compared to natural gas.

Table 7. Compositional benchmark of synthetic fuel and natural gas

Symbol	Compound	Compositions (%)	
		This study	Natural Gas [13]
CH ₄	Methane	32.9	70-98
C ₂ H ₆	Ethane	16.5	1-10
C ₃ H ₈	Propane	24.7	0-5
C ₃ H ₆	Propylene	0.99	-
C ₄ H ₁₀	Butane	17.4	0-2
C ₄ H ₈	Butene	2.37	-
CO ₂	Carbon dioxide	3.81	0-1
O ₂	Oxygen	1.07	0-0.2
N ₂	Nitrogen	0.36	0-15
H ₂ S	Hydrogen sulfide	-	Trace occasionally
H ₂ O, H ₂ , He	Rare gases	0.01	Trace occasionally

Fuel quality is another key point to concentrate on. The calorific value is an essential characteristic used to evaluate fuel quality. The calorific value of a fuel can be measured using the bomb calorimetry and the standard methods such as ASTM-D201. In addition, some estimation equations were suggested to determine the heating value based on the elemental compositions of hydrocarbons [43]. As a result of the evaluation, gross and net calorific values of the produced synthetic fuel and comparison with other common fuel types are illustrated in Fig. 5 [13–42]. The gross calorific value of a fuel is equal to the net calorific value with the addition of the heat of vaporization of the water content in the fuel. The synthetic fuel produced was found to be a fuel

type, an immensely qualified fuel, compared with other types of fossil fuels.

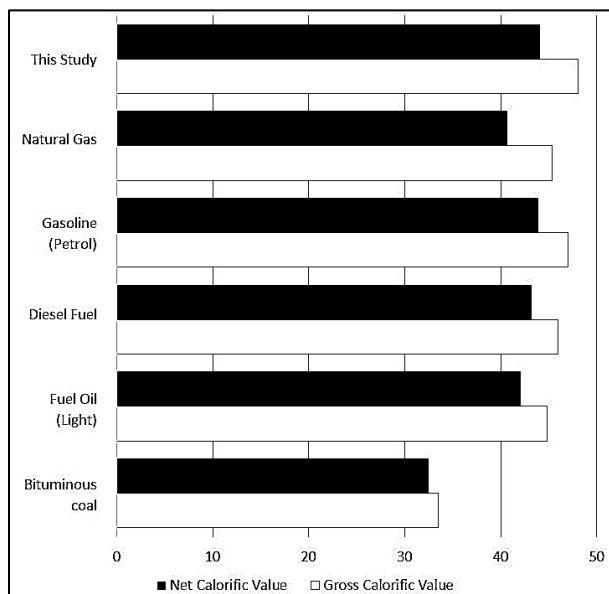


Figure 5. Calorific values of various fuels (MJ/kg) [13, 42].

Economic analysis

A preliminary economic analysis was calculated based on the engineering economic analysis of Turton

Table 8. Total operating cost

	Expenses	Percentage %	Calculated Values (\$M)
CTM	Equipment Costs		63.3
	Coolers	2.09 of FCI _L	1.64
	Heaters	2.47 of FCI _L	1.94
	Compressors	48.1 of FCI _L	37.7
	Reactors	2.88 of FCI _L	2.26
	Furnaces	26.0 of FCI _L	19.7
WC	Working Capital	15.0 of FCI _L	11.8
L	Land Cost	1.00 of FCI _L	0.79
FCI	Fixed Capital Investment		78.5
C _{OL}	Operating Labor	1.43 of COM _d	1.42
C _{UT}	Utility Costs		18.1
	Coolers	0.64 of COM _d	0.61
	Heaters	1.33 of COM _d	1.27
	Compressors	0.03 of COM _d	0.03
	Furnaces	16.8 of COM _d	16.1
C _{RM}	Raw Materials		45.2
	Flue Gas	-	-
	Hydrogen	47.2 of COM _d	45.2
COM	Total Manufacturing Cost		95.8

et al. [44]. The detailed equipment purchased and production costs were calculated by assuming Chemical Engineering Plant Cost Index (CEPCI) as 500. Land cost and working capital were assumed as 1% and 15% of the fixed capital investment, respectively [45]. The cost of nitrogen gas was taken as \$0.08/kg [46], and the price of synthetic fuel was assumed to be the same as the price of natural gas. The capital cost of each piece of equipment was calculated as \$63,790,535, and it was used to determine the fixed capital investment, FCI, of the project. FCI refers to an entirely new facility in which the construction was started on an essentially undeveloped area, a grass field. Besides, working capital is required to start up the plant and finance the first few months of operation. The total operating cost of the process is shown in Table 8. The cost of manufacturing is the sum of costs of all resources consumed in making products, and the result of COM is \$95,980,622. There are four categories to achieve theoretical manufacturing cost, COM. These were shown in Eq. (14).

$$\text{COM} = 0.18\text{FCI} + 2.73\text{C}_{\text{OL}} + 1.23(\text{C}_{\text{UT}} + \text{C}_{\text{WT}} + \text{C}_{\text{RM}}) \quad (14)$$

The first category is the cost of operating labor, C_{OL} , calculated from the amount of equipment in the plant. Hence, 15 operating laborers were determined, and C_{OL} is \$1,134,137. Then, the second category is the utility expenses, C_{UT} . Those utilities are low-pressure steam, nitrogen refrigerator, natural gas, and electric power consumed throughout the process. The third category is the cost of raw materials (C_{RM}). Since the purchase price of flue gas was assumed to be zero, only hydrogen was included in raw material expenses. Finally, C_{WT} stands for the cost of waste treatments. However, there is no waste material in the stream. The purge stream was composed of hydrogen-rich gases. Therefore, it can be incinerated or used as process fuel.

There are three bases used for the profitability analysis of plant design. These are time, cash, and interest rate criteria. Considering Europe's average corporate income tax rate (22.5 percent) [47], which is slightly higher than the global average (21.4 percent) and a discount rate (10 percent), the time and interest rate criteria were only considered in this study. The term used for the time criterion is the payback period (PBP). It is the time required to recover the capital investment. The project's PBP and discounted payback period (DPBP) were calculated as 6.1 and 7.5 years, respectively. The rate of return on investment (ROROI) was also used as an interest rate criterion in this economic estimation, and it was calculated as 16.64%.

Sustainable development goals

The Sustainable Development Goals (SDGs) or Global Goals are a collection of 17 interlinked goals designed to be a "blueprint for achieving a better and more sustainable future for all" by the United Nations Development Programme (UNDP) [48]. The excess water can be sold to industrial production facilities to avoid using natural water sources. Thus, clean water and sanitation (goal 6) can be provided. Also, synthetic fuel was produced, an affordable and clean energy source (goal 7, aimed to be achieved by 2030 by UNDP). Supporting sustainable industries and investing in R&D are significant ways to provide sustainable growth; thus, goal 9 (industry, innovation, and infrastructure) was also fulfilled. The study's objective is to protect natural resources related to goal 12 (responsible consumption and production). Since CO_2 emission serves climate change, climate action (goal 13) was provided. Finally, ocean acidification will be reduced by reducing CO_2 emissions. Hence, the aquatic living beings will be protected.

CONCLUSION

Fossil energies (FE) will remain the mainstay of

global energy consumption for the future based on their current superiority [49]. 41% of all anthropogenic CO_2 emissions will derive from industrial power plants by 2035. Environmental problems caused by GHG emissions are directly associated with nonrenewable energy production and utilization. Hence, studying potential energy systems is fundamental for preventing future climate change caused by humankind. For instance, carbon pricing is one of the most effective ways to reduce emissions, which manages GHG emissions by placing a fee on emitting and offering an incentive for emitting less by 2025. This action shifts in consumption and investment patterns, making economic development compatible with climate protection [50].

Substituting FEs with renewable energy has an essential role in developing a sustainable and carbon-free economy. Thus, this study aims to develop an alternative sustainable flue gas-to-fuel recycle system to cut down the dependence on FEs. Fischer-Tropsch synthesis is used to produce the hydrocarbon mixture from syngas. Since CO_2 has a negative impact on the Fischer-Tropsch process due to reducing the selectivity of hydrocarbons with carbon numbers above 5 [51], the excess CO_2 gas is distinguished after the reverse water gas shift reaction and before the Fischer-Tropsch synthesis. $FeCuK/Al_2O_3$ catalyst is 600 °C for the Fischer-Tropsch synthesis in R-203 to produce hydrocarbons whose carbon number is up to 4. $FeCuK/Al_2O_3$ catalyst also provided a high CO conversion rate (98.4%) and high hydrocarbon selectivity (88%). The produced synthetic fuel has a gross calorific value of 48 MJ/kg, which is effective compared with other FEs. About 6.59% of the input components are converted into synthetic fuel, while other parts are distinguished as 90.3% pure nitrogen gas (71.6%), excess industrial water (19.4%), and elemental sulfur (0.05%). The remained part (about 2.4%) of the input streams is disposed of as the purge stream (Fig. 3).

Equipment and utility costs are calculated regarding the types and properties of equipment operating in the simulation. The raw material H_2 occupies a major part of the cost of manufacturing. Thus, this process may be combined with H_2 production technologies. The electrochemical methods for H_2 production, such as electrolysis or photoelectrochemical, may be adapted to convert excess water distinguished from the system to H_2 . Although these technologies may be the cleanest ones, they cost around 80% of the operating cost and are highly expensive. Besides, photosynthetic processes (including algae) which use CO_2 and H_2O for H_2 production are also sustainable technologies [52].

The payback period is calculated as 6.1 years, while discounted payback period is about 7.5 years, concerning the discount rate of 10%. Therefore, ROROI is also measured as 16.64%, which can be considered a good ROROI for an investment [53].

REFERENCES

- [1] UN Environmental Programme, UN Environment Annual Report 2019, <https://www.unep.org/annualreport/2019/index.php> [accessed 16 September 2020].
- [2] National Oceanic and Atmospheric Administration, Ocean acidification, <https://www.noaa.gov/education/resource-collections/ocean-coasts/ocean-acidification> [accessed 16 September 2020].
- [3] F. Stocker, K. Qin, M. Plattner, K. Tignor, J. Allen, A. Boschung, V. Xia, Climate Change: The Physical Science Basis, in Intergovernmental Panel on Climate Change, Geneva, Switzerland (2013), p. 190–196.
- [4] Global Climate Change - Facts (FAQ). NASA - Climate Change: Vital Signs of the Planet. Retrieved February 20, 2021, from <https://climate.nasa.gov/faq/>.
- [5] Minnesota Pollution Control Agency, Chlorofluorocarbons (CFCs) and hydrofluorocarbons (HFCs), <https://www.pca.state.mn.us/air/chlorofluorocarbons-cfcs-and-hydrofluorocarbons-hfcs> [accessed 20 November 2020].
- [6] T. Gunduz, Environmental Chemistry, Gazi Publishers, Ankara (2012), p. 90–170.
- [7] R. Kolieb, D. Herr, Clim. Policy, 12 (2011) 378–389.
- [8] B. Bereiter, S. Eggleston, J. Schmitt, C. Ahles, F. Stocker, H. Fischer, S. Kipfstuhl, J. Chapellaz, Geophys. Res. Lett. 42 (2015) 542–549.
- [9] M. Ozturk, I. Dincer, Nat. Gas Sci. Eng. 83 (2020) p. 103–111.
- [10] International Energy Agency Statistics, CO2 emissions statistics, <https://www.iea.org/data-and-statistics/data-product/co2-emissions-from-fuel-combustion-highlights#overview> [accessed 16 July 2021].
- [11] United Nations Environment Programme, Lagging in climate action, G20 nations have huge opportunities to increase ambition, <https://www.unep.org/news-and-stories/press-release/lagging-climate-action-g20-nations-have-huge-opportunities-increase> [accessed 17 April 2021].
- [12] J. Olivier, W. Peters, Trends in Global CO2 and Total Greenhouse Gas Emissions, https://www.pbl.nl/sites/default/files/downloads/pbl-2020-trends-in-global-co2-and-total-greenhouse-gas-emissions-2019-report_4068.pdf [accessed 18 April 2020].
- [13] G. Speight, Natural Gas: A Basic Handbook, Gulf Professional Publishing, London (2019), p. 59–98.
- [14] E. Koohestanian, F. Shahraki. J. Environ. Chem. Eng. 9(4) (2021), 105–125.
- [15] M. A. Nemitallah, M. A. Habib, H. M. Badr, S. A. Said, A. Jamal, R. Ben-Mansour, E. M. A. Mokheimer, K. Mezghani. Int. J. Energy Res. 41(12) (2017), 1670–1708.
- [16] X. Liang, Q. Wang, Z. Luo, H. Zhang, K. Li, Y. Feng, R. Shaikh, J. Cen, RSC Adv. 8 (2018) 35690–35699.
- [17] S. Abuelgasim, W. Wang, A. Abdalazeez, Sci. Total Environ. 764 (2021) 142–892.
- [18] M. Osman, N. Khan, A. Zaabout, S. Cloete, S. Amini. Fuel Process. Technol. 214 (2021) 106–684.
- [19] A. K. Vuppaladadiyam, J. G. Yao, N. Florin, A. George, X. Wang, L. Labeeuw, Y. Jiang, R. W. Davis, A. Abbas, P. Ralph, P. S. Fennell, M. Zhao. ChemSusChem. 11(2) (2018), 334–355.
- [20] R. Kothari, S. Ahmad, V. V. Pathak, A. Pandey, A. Kumar, R. Shankarayan, P. N. Black, V. V. Tyagi. Biomass Convers. Biorefin. 11(4) (2019) 1419–1442.
- [21] E. Koohestanian, J. Sadeghi, D. Mohebbi-Kalhari, F. Shahraki, A. Samimi. Energy, 144 (2018) 279–285.
- [22] P. Ortega, Analyzes of Solar Chimney Design, Trondheim, Norway (2011), p. 78.
- [23] A. Simonovic, N. Stupar, P. Pekovic, FFME Trans. 36 (2008) 119–125.
- [24] R. Arachchige, C. Melaaen, Energy Procedia. 23 (2012) 391–399.
- [25] Process Instrumentation Consultancy & Design, & Edwards, J. E. Process Modelling Selection of Thermodynamic Methods. Chemstations. (2018) https://www.chemstations.com/content/documents/Technical_Articles/thermo.pdf.
- [26] D. Aaron, C. Tsouris, Sep Sci Technol. 40 (2005) 321–348.
- [27] J. Mustafa, M. Farhan, M. Hussain, J. Membr. Sci. 6 (2016) 221–238.
- [28] F. Russo, F. Galiano, A. Iulianelli, A. Basile, A. Figoli, Fuel Process. Technol. 213 (2021) 106–643.
- [29] I. Song, H. Ahn, H. Jeon, K. Jeong, Y. Lee, H. Choi, H. Kim, B. Lee, Desalination, 234 (2008) 307–315.
- [30] G. Towler, R. Sinnott, Chemical Engineering Design: Principles, Practice and Economics of Plant and Process Design, Elsevier, Amsterdam (2012) p. 811–816.
- [31] D. Kundnane, K. Kushwaha, 2015, A Critical Review on Heat Exchangers used in Oil Refinery, in 3rd Afro-Asian International Conference on Science, Engineering and Technology, Bharuch, India (2015), p. 1–5.
- [32] M. Rhine, S. Truelove, HEDH Multimedia-Heat Exchanger Design Handbook, Begell House Inc. Connecticut (2014) p. 24.
- [33] International Organization for Standardization, Petroleum Product-Determination of sulfur content of automotive fuels—Ultraviolet fluorescence method (ISO 20846:2019), <https://www.iso.org/standard/74313.html> [accessed 17 April 2020].
- [34] N. Mashapa, D. Rademan, J. Vuuren, Ind. Eng. Chem. Res. 46 (2007) 6338–6344.
- [35] J. Zaman, A. Chakma, Fuel Process. Technol. 41 (1995) 159–198.
- [36] A. Wolf, A. Jess, C. Kern, Chem. Eng. Technol. 39 (2016) 1040–1048.
- [37] H. Kang, W. Bae, Y. Cheon, J. Lee, S. Ha, W. Jun, H. Lee, W. Kim, Appl. Catal. B. 103 (2011) 169–180.
- [38] J. Chang, L. Bai, T. Teng, L. Zhang, J. Yang, Y. Xu, W. Xiang, W. Li, Chem. Eng. Sci. 62 (2007) 4983–4991.
- [39] A. Delparish, A. K. Avci. Fuel Process. Technol. 151 (2016) 72–100.
- [40] Y. N. Wang, W. P. Ma, Y. J. Lu, J. Yang, Y. Xu, H. W. Xiang, Y. Li, Y. L. Zhao, B. J. Zhang. Fuel, 82 (2021) 195–213.
- [41] H. Brauers, I. Braunger, J. Jewell, Energy Res. Soc. 76 (2021) 102–120.
- [42] J. Carvill, Mechanical Engineers Data Handbook, M. Kutz Ed., Elsevier, Amsterdam (2005), 102–145.
- [43] S. Hosokai, K. Matsuoka, K. Kuramoto, Y. Suzuki, Fuel Process. Technol. 152 (2016) 399–405.
- [44] R. Turton, J. Shaeiwitz, D. Bhattacharyya, W. Whiting, Analysis, Synthesis, and Design of Chemical Processes (International Series in the Physical and Chemical

- Engineering Sciences), Pearson, London (2018), 156–213.
- [45] R. Woods, Rules of Thumb in Engineering Practice, Wiley, New York (2007).
- [46] J. Kim, Y. Seo, D. Chang, *Apl. Energy*. 182 (2016) 154–163.
- [47] E. Asen, Corporate Income Tax Rates in Europe, <https://taxfoundation.org/2020-corporate-tax-rates-in-europe> [accessed 16 April 2020].
- [48] United Nations Development Programme, Sustainable Development Goals, <https://sdgs.un.org/goals> [accessed 16 September 2020].
- [49] M. Höök, X. Tang. Depletion of fossil fuels and anthropogenic climate change—A review. *Energy Policy*, 52 (2013) 797–809.
- [50] United Nations Framework Convention on Climate Change. About Carbon Pricing, <https://unfccc.int/about-us/regional-collaboration-centres/the-ci-aca-initiative/about-carbon-pricing#eq-1> [accessed 8 February 2022].
- [51] W. C. Wang, Y. C. Liu, R. A. A. Nugroho, R. A. A. Energy, 239 (2022) 121970.
- [52] R. Chaubey, S. Sahu, O. James, S. Maity. *Renew. Sust. Energy. Rev.* 23 (2013) 443–462.
- [53] Birken, E. G. Understanding Return on Investment (ROI). *Forbes Advisor*, <https://www.forbes.com/advisor/investing/roi-return-on-investment/> [accessed 9 February 2022].

H. BATUHAN OZTEMEL
INCI SALT
YAVUZ SALT

Department of Chemical
Engineering, Faculty of Chemical
and Metallurgical, Yildiz
Technical University, Istanbul,
Turkey

NAUČNI RAD

KORIŠĆENJE UGLJEN-DIOKSIDA: SIMULACIJA PROCESA PROIZVODNJE SINTETIČKOG GORIVA IZ DIMNIH GASOVA

Problemi životne sredine su u porastu i danas više povezani sa klimom, prvenstveno uzrokovani emisijom gasova sa efektom staklene bašte. Takođe, industrijske emisije širom sveta iz elektrana će prouzrokovati 50% koncentracije ugljen-dioksida u atmosferi do 2035. godine. Za simulaciju proizvodnje sintetičkog goriva iz dimnih gasova koje emituju industrijske elektrane korišćen je softver ChemCAD. Ona je imala za cilj da sve sastojke dimnih gasova konvertuje u vredne proizvode kako bi se smanjio uticaj štetnih gasova na životnu sredinu. Proizvedeno sintetičko gorivo sastoji se od 94,75% ugljovodonika sa brojem ugljenika do četiri sa ukupnom stepenom konverzije od 6,59%. Oko 95% sumpora u dimnom gasu se izdvaja odsumporavanjem smeše goriva. Membranski proces, takođe, izdvaja 90,3% azota iz dimnog gasa. Sumporizacijom, povratnom reakcijom vod-gas i Fišer-Tropšovom sintezom u prisustvu sa odgovarajućih katalizatora postižu se stepeni konverzije od 95%, 79% i 98,4% u jednom prolazu, reodm. Urađena je i ekonomska analiza, a period otplate projekta je 6,1 godina, dok je zarada na investirano 16,64%.

Ključne reči: ugljen-dioksid, Fišer-Tropšova sinteza, dimni gas, simulacija procesa, sintetičko gorivo.

